Supporting Information

A Lightweight and Ultrastrong Polymer Foam with Unusually Superior Flame Retardancy

Linli Xu,[†] Linhong Xiao,[†] Pan Jia,[†] Karel Goossens,[‡] Peng Liu,[∏] Hui Li,[†] Chungui Cheng,[†] Yong Huang,[†] Christopher W. Bielawski,[‡,§] and Jianxin Geng[†]*

[†] Technical Institute of Physics and Chemistry, Chinese Academy of Sciences, 29 Zhongguancun East Road, Haidian District, Beijing 100190, P. R. China, Email: jianxingeng@mail.ipc.ac.cn

[‡] Center for Multidimensional Carbon Materials (CMCM), Institute for Basic Science (IBS), Ulsan 44919, Republic of Korea

[§] Department of Chemistry and Department of Energy Engineering, Ulsan National Institute of Science and Technology (UNIST), Ulsan 44919, Republic of Korea

[∏] Beijing National Laboratory for Molecular Science, CAS Key Laboratory of Engineering Plastics, Institute of Chemistry, Chinese Academy of Sciences, Beijing 100190, P. R. China

CONTENTS:

1. Morphological and compositional data of the GPx composites

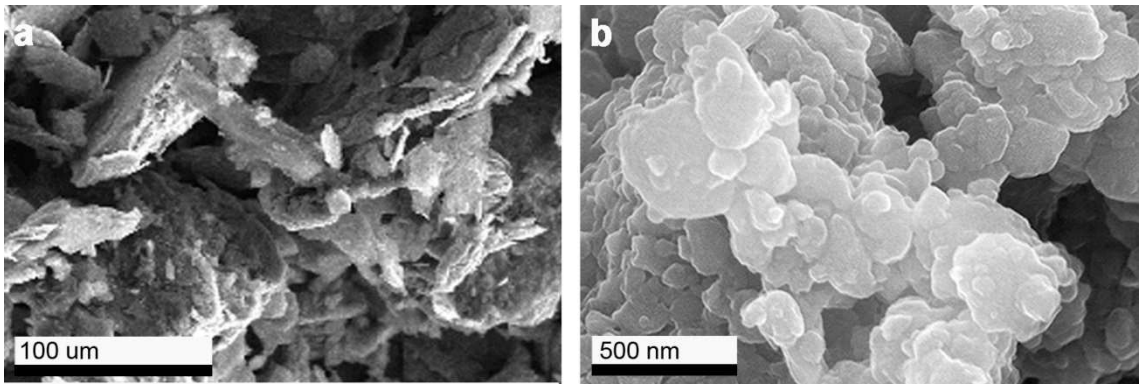

Figure S1. SEM images of (a) graphite and (b) GP2 composite.

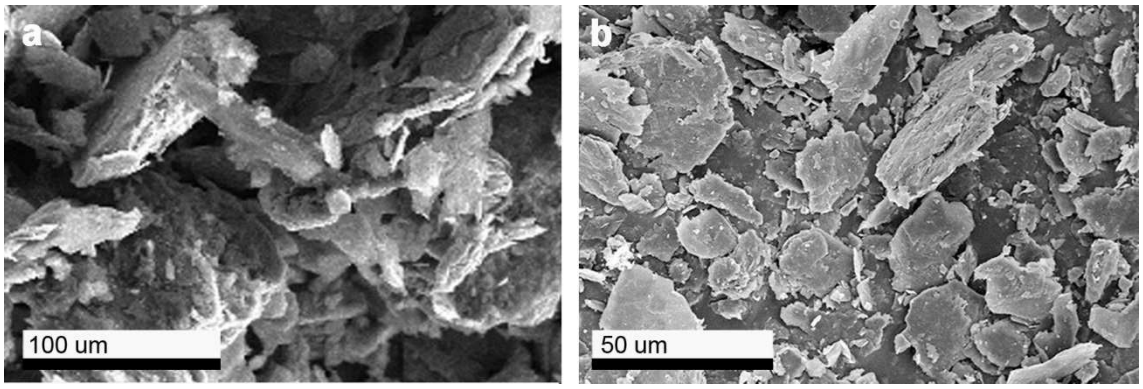

Figure S2. SEM images of graphite (a) before and (b) after ball milling.

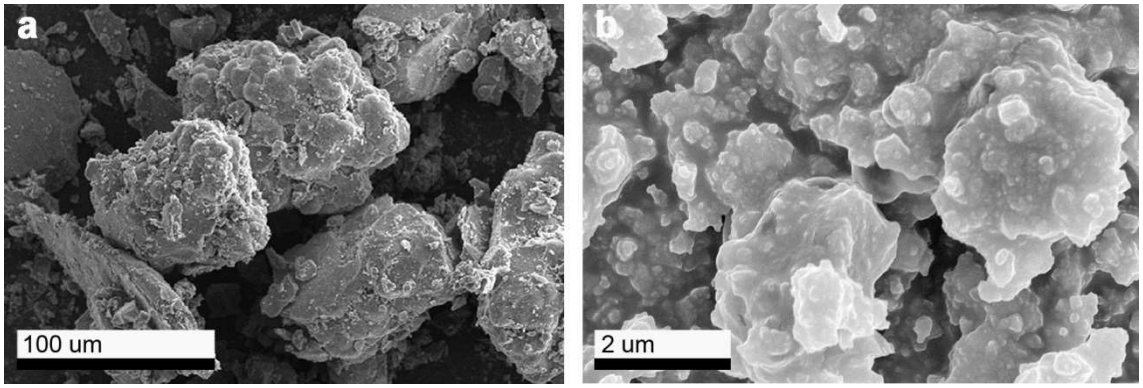

Figure S3. SEM images of RP (a) before and (b) after ball milling.

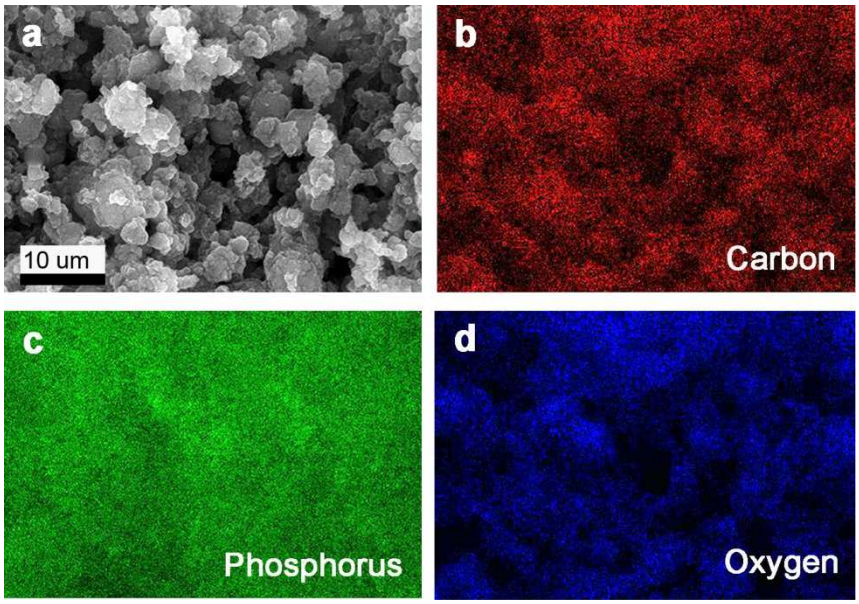

Figure S4. EDS elemental mapping data of GP2. (a) An SEM image of GP2. (b–d) EDS elemental maps of (b) carbon, (c) phosphorus and (d) oxygen, which were collected from the entire area shown in a.

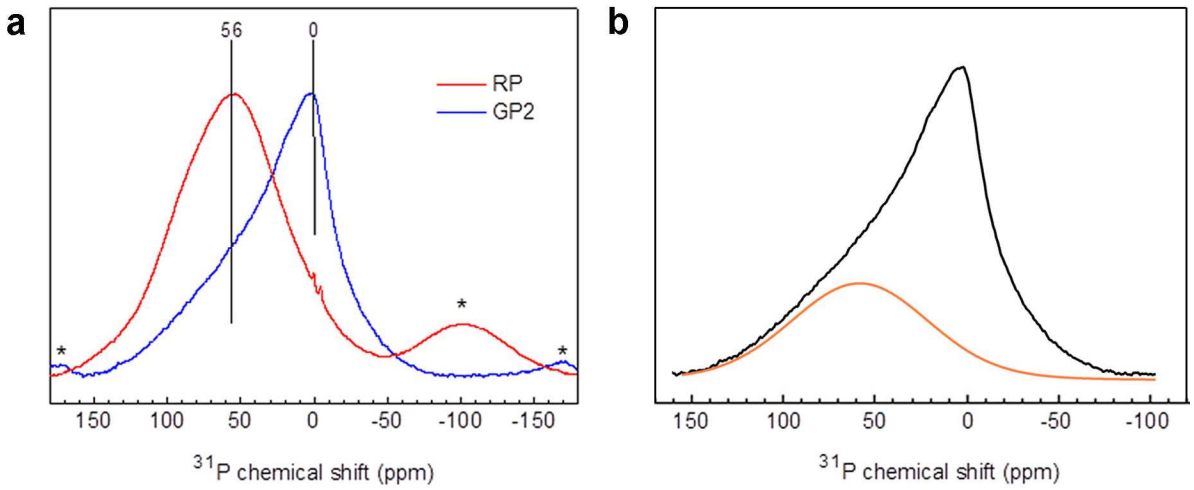

Figure S5. (a) Solid-state ^{31}P MAS NMR spectra of pristine RP and GP2. The spinning sidebands are indicated by asterisks. (b) The ^{31}P MAS NMR spectrum of GP2 and a deconvoluted a signal that is consistent with the presence of RP.

Solid-state ^{31}P MAS NMR spectra were collected on a Bruker Avance III HD 11.7 T wide-bore spectrometer, operating at a ^{1}H NMR frequency of 500.31 MHz and a ^{31}P NMR frequency of 202.53 MHz. For the ^{31}P direct pulse MAS NMR measurements, a Bruker triple-resonance MAS NMR probe (MASDVT500W2 BL1.9) was used, with 1.9 mm diameter rotors made of ZrO_2 barrels and Vespel® end caps. The magic angle was set using the ^{79}Br resonance of KBr. ^{31}P chemical shifts were referenced to 85% H_3PO_4 (δ = 0 ppm) via the external secondary standard ammonium dihydrogen phosphate at δ = 1.00 ppm.[1,2] A spinning frequency of 35 kHz was employed for all samples. For each sample, a 90° ^{31}P pulse was applied with a relaxation delay of 600 seconds to ensure full spin relaxation. For the measurements of GP2, GP4 and GP6, a total of 64 scans were averaged and Fourier transformed with 200 Hz line broadening to obtain each spectrum. For the analysis of RP, a total of 32 scans were averaged and Fourier transformed with 200 Hz line broadening to obtain the spectrum.

The ^{31}P MAS NMR spectrum of the same batch of pristine RP used in this research contains a very broad band centered at ~56 ppm (Figure S5a) and is in agreement with literature reports.[3-6] Hybridization of graphene platelets with RP obtained through ball milling is reflected by the evolution of the ^{31}P MAS NMR spectra of GP2 (Figure S5a). While the signal centered at ~0 ppm can be ascribed to phosphonic acid groups,[3,7] the broad downfield shoulder centered at ~56 ppm, which was also observed after deconvolution (Figure S5b), can be ascribed to RP. The broad signal of the RP is due to strong ^{31}P–^{31}P homonuclear dipolar interactions and ^{31}P chemical shift anisotropy.

Table S1. Total acidity[a] of the GPx composites and the products obtained after full oxidation.[b]

Sample	A_O [mmol g^{-1}][c]	A_T [mmol g^{-1}][d]	A_O : (A_T–A_O)[e]
GP2	4.97	18.67	1 : 2.77
GP4	4.37	23.50	1 : 4.38
GP6	3.46	23.98	1 : 5.39

[a]Total acidity of the GPx composites before and after full oxidation was determined by a back titration method.[8,9] [b]Full oxidation of the GPx composites was performed at 350 °C in air until a maximum increase in mass was obtained, and ascribed to the full transformation of RP into P_2O_5. [c]Before oxidation, the total acidity (A_O) represents the quantity of phosphonic acid groups attached to the edges of graphene platelets. [d]After full oxidation, the total acidity (A_T) obtained reflects all phosphorus species, including those that exist in various oxidized states as well as elemental phosphorus in the GPx composites. The A_T is represented with respect to the mass of the GPx composites before oxidation. [e]A_O : (A_T–A_O) represents the mole ratio of oxidized phosphorus relative to the elemental phosphorus in the GPx composites.

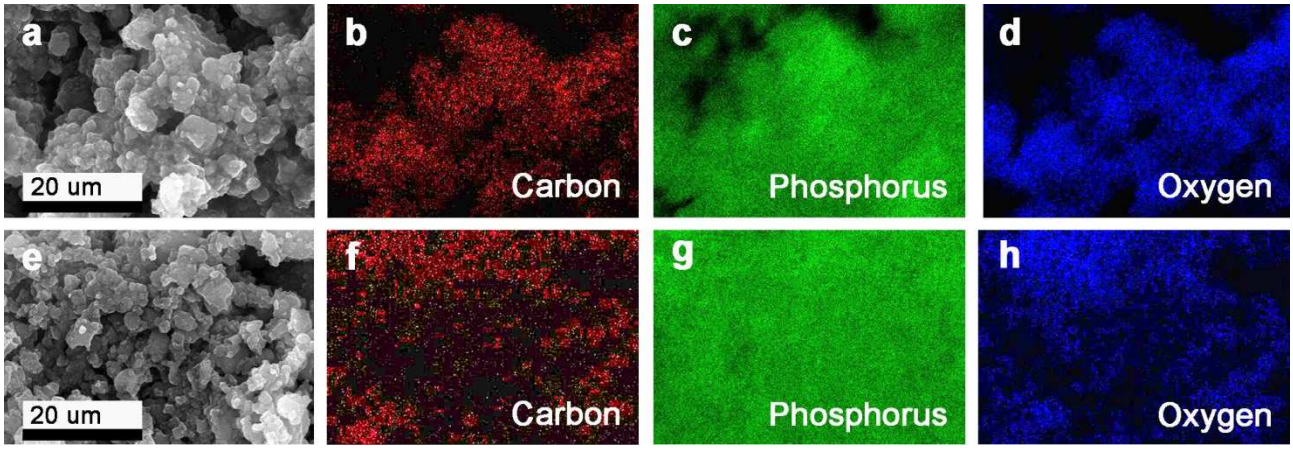

Figure S6. EDS elemental mapping data of GP4 and GP6. (a) An SEM image of GP4. (b–d) EDS elemental maps of (b) carbon, (c) phosphorus and (d) oxygen, which were collected from the entire area shown in a. (e) An SEM image of GP6. (f–h) EDS elemental maps of (f) carbon, (g) phosphorus and (h) oxygen, which were collected from the entire area shown in e.

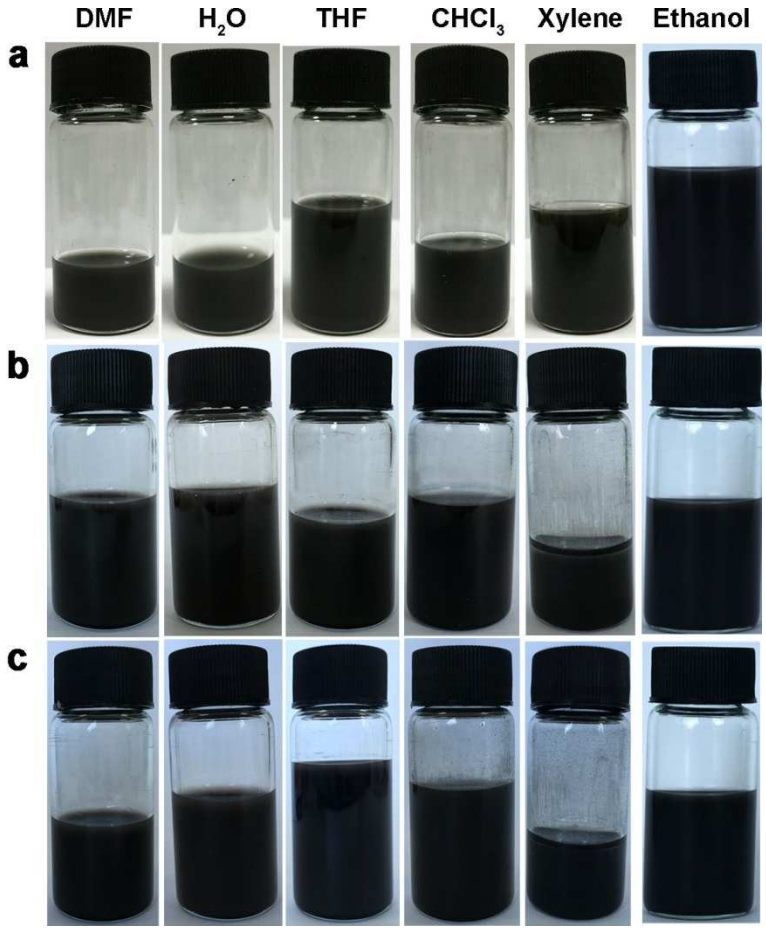

Figure S7. Photographs of suspensions of the GPx composites in various solvents (indicated). (a) GP2, (b) GP4 and (c) GP6. The concentrations of the GPx composites in the respective suspensions were 0.5 mg mL^{-1}.

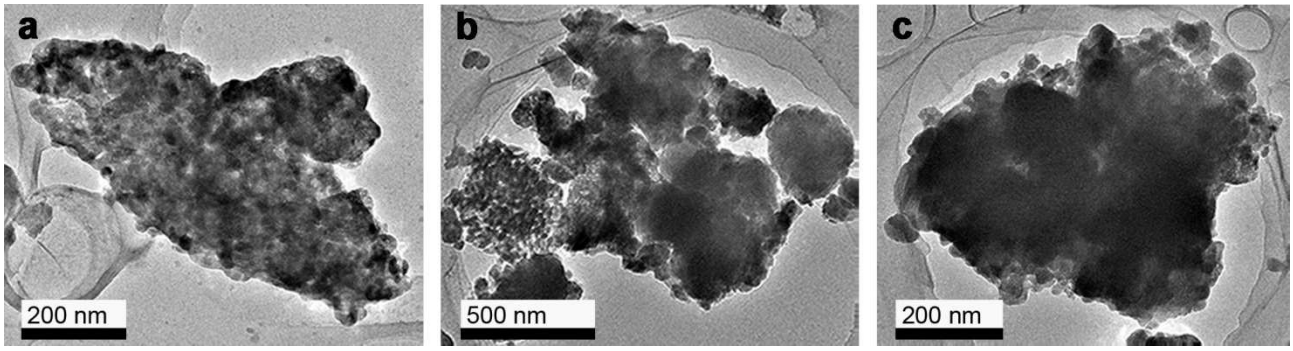

Figure S8. TEM images of (a) GP2, (b) GP4 and (c) GP6.

2. Preparation and characterization additional data of the isocyanate-based PI foams

Part I

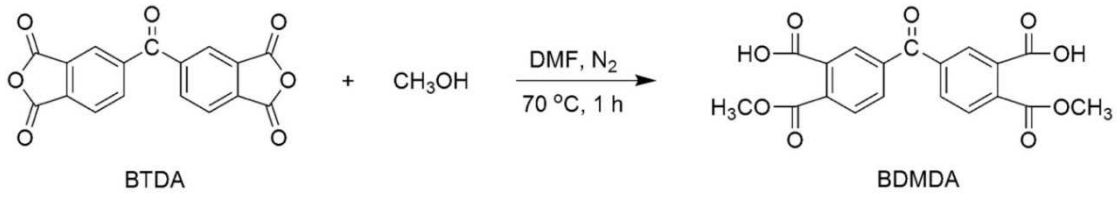

Part II

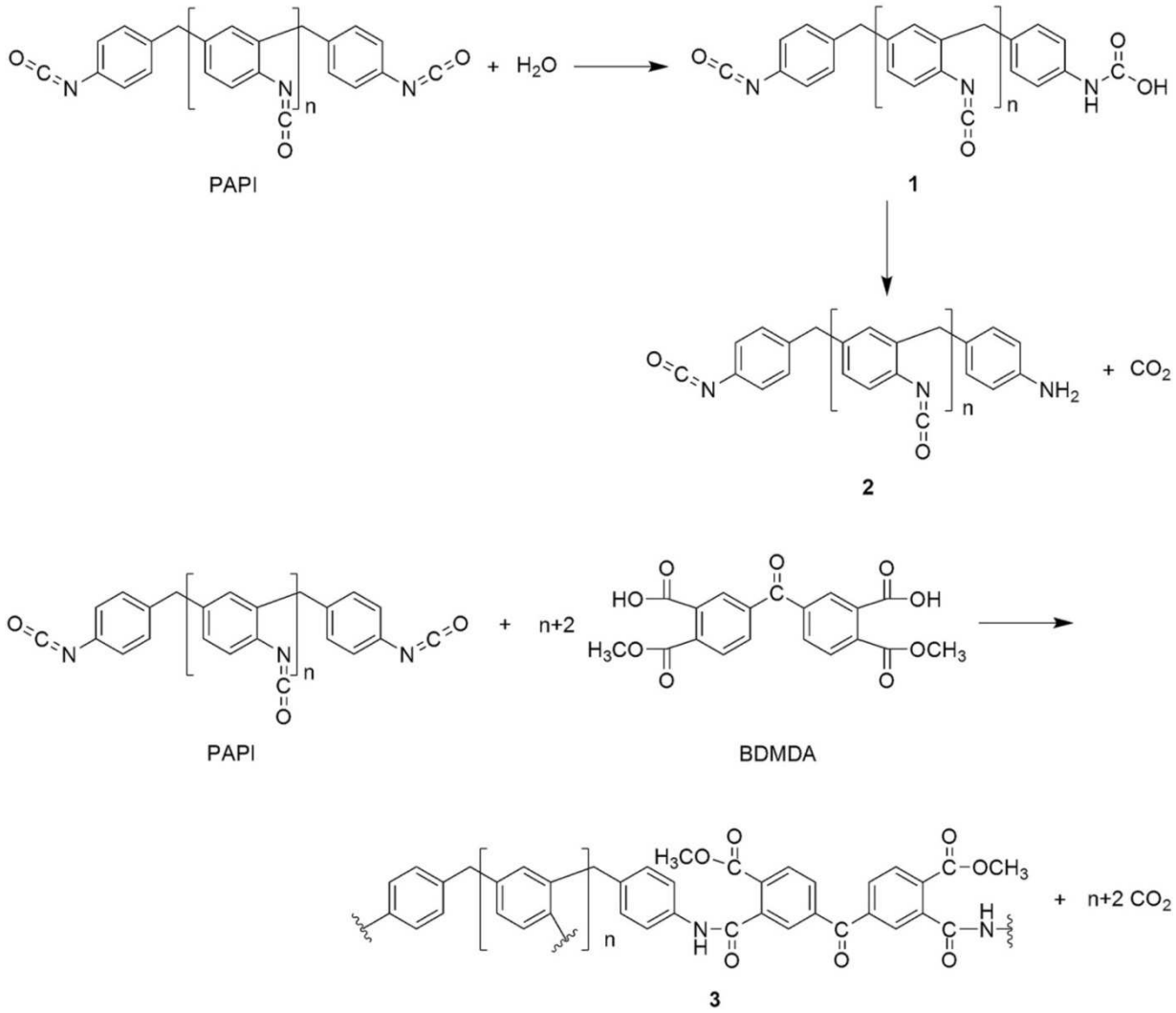

To be continued.

Continued.

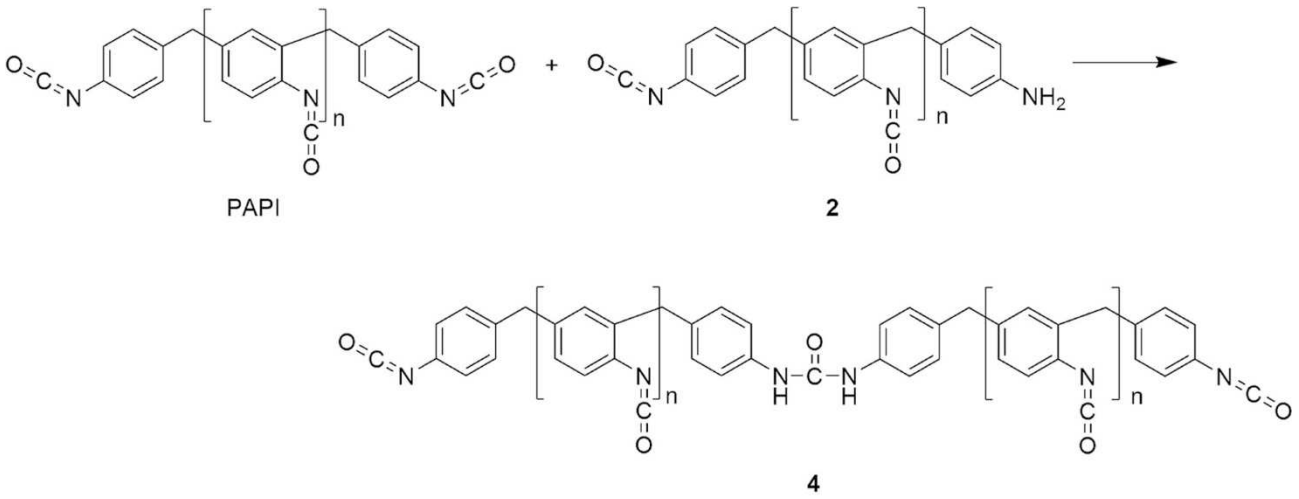

Part III

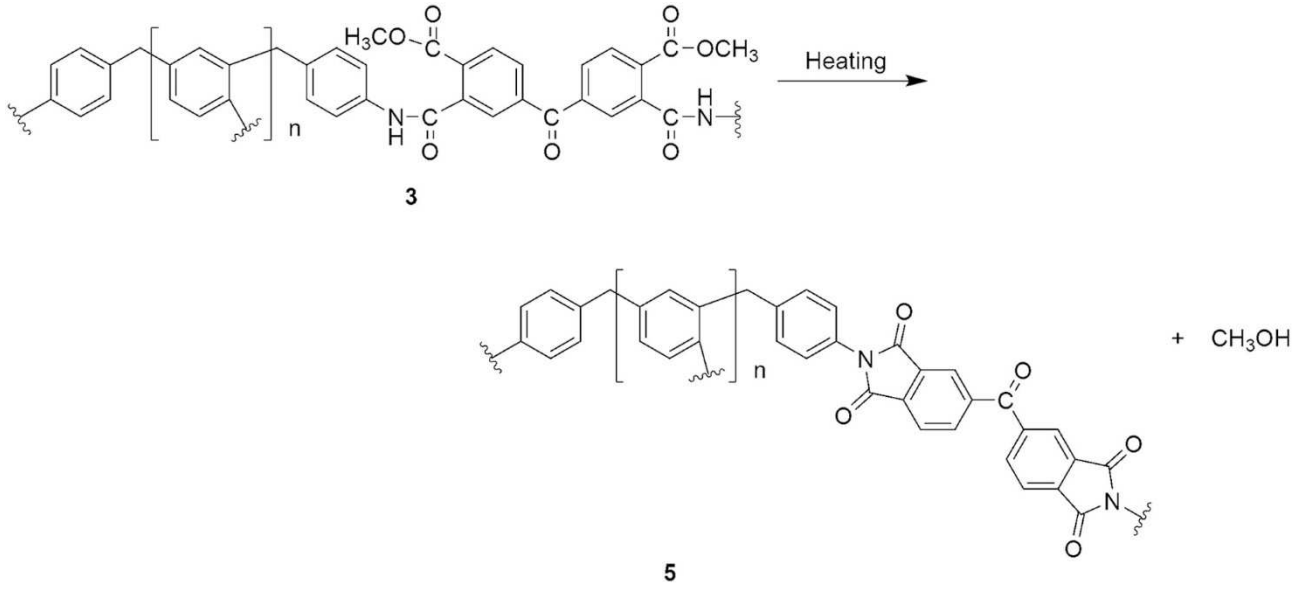

Scheme S1. Foam formation chemistry. **Part I:** Synthesis of BDMDA. **Part II:** Chemical reactions that may occur during foam formation. **Part III.** Chemical reactions that may occur during condensation.

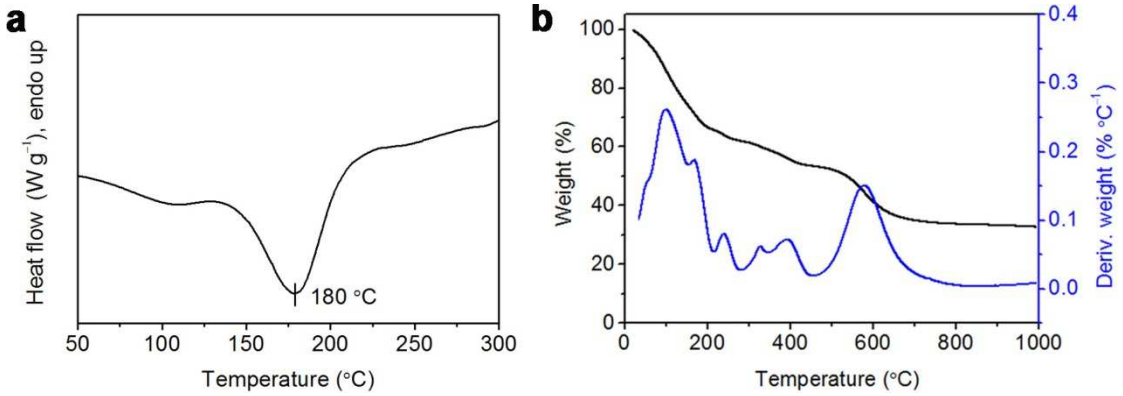

Figure S9. Thermal analysis of the PI precursor foams. (a) DSC and (b) TGA data. DSC data were collected on a Mettler Toledo DSC1 Star System at a scanning rate of 10 °C min^{-1} under an atmosphere of N_2.

To determine the conditions for the thermal conversion of the PI precursor foams to the PI foams, DSC and TGA data of the former were collected (Figure S9). In the DSC curve, a significant exothermal peak was detected from ca. 150 to 225 °C with a maximum at 180 °C. This exothermal peak was attributable to imidization. Similarly, TGA revealed a weight loss due to release of volatile molecules over the same temperature range. Based on these results, the PI precursor foams were thermally treated at 180 °C for 2 h and then at 250 °C for 1 h to facilitate imidization.

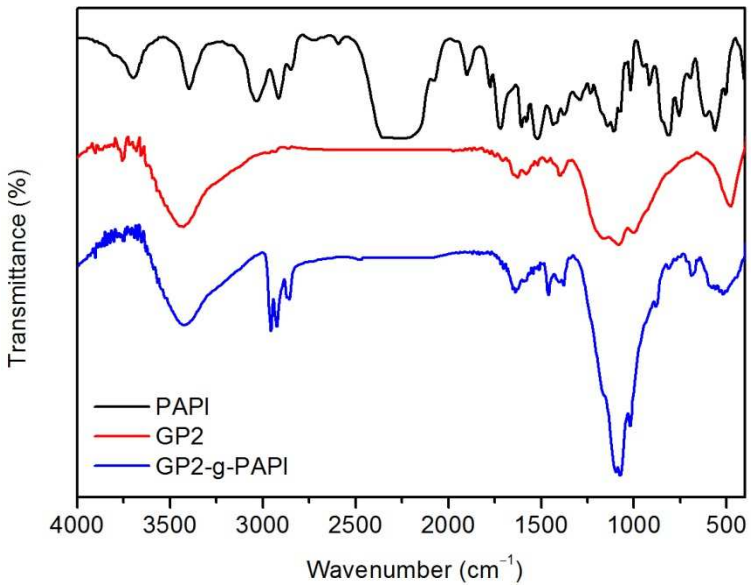

Figure S10. FT-IR spectra recorded for PAPI, GP2 and GP2-g-PAPI (see text below).

A GP2 composite was grafted with PAPI and designated as GP2-g-PAPI by stirring a mixture of GP2 and PAPI (1:4 in mass) in DMF at 70 °C for 2 h. The product was separated by cycles of centrifugation and washing with DMF, and then dried and finally characterized using FT-IR spectroscopy (Figure S10). Strong signals at 1022, 1078 and 1099 cm^{-1} as well as a group of weak but sharp signals near 2900 cm^{-1} were found in the FT-IR spectrum recorded for GP2-g-PAPI. Such spectroscopic features are consistent with covalent crosslinking between GP2 platelets and the polymer matrix.

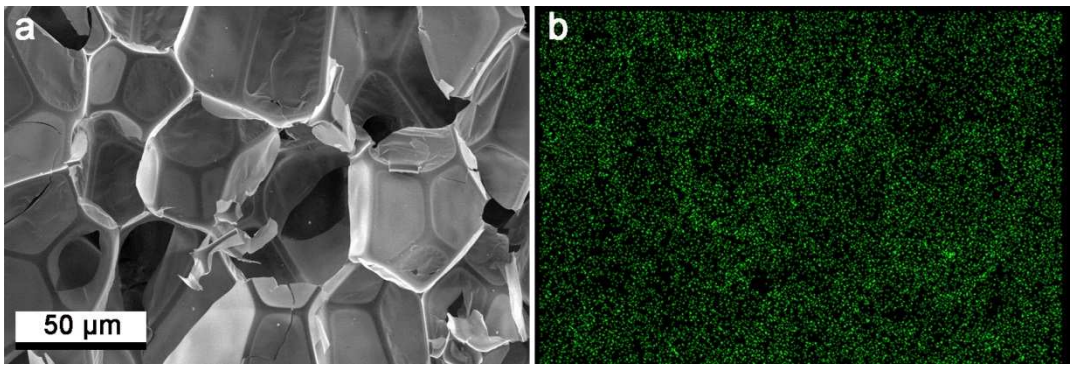

Figure S11. EDS elemental mapping data of a PI foam containing 2.2 wt% of GP2. (a) An SEM image of the PI foam containing 2.2 wt% of GP2. (b) EDS elemental map of phosphorus, which was collected from the entire area shown in a. The uniform distribution of phosphorus indicated that GP2 was well dispersed in the polymer matrix.

Table S2. Densities of pristine PI foam and the PI foams containing 2.2 wt% of the various additives (indicated).

Sample	Pristine PI foam	PI foam 2.2 wt% graphite	PI foam 2.2 wt% RP	PI foam 2.2 wt% GP2	PI foam 2.2 wt% GP4	PI foam 2.2 wt% GP6
Density [g cm^{-3}]	0.020±0.005	0.022±0.003	0.018±0.002	0.016±0.001	0.016±0.002	0.017±0.002

3. Additional flame-retardant data of the various PI foams

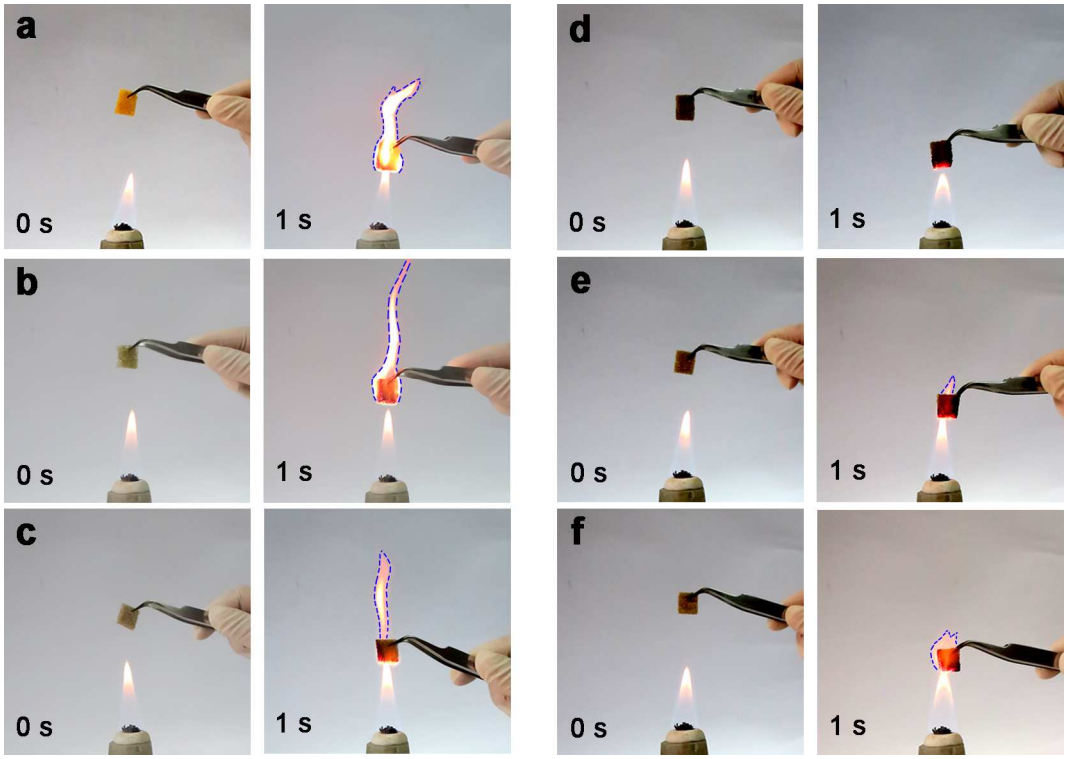

Figure S12. Combustion progress of various PI foams. (a) Pristine PI foam. (b–f) The PI foams containing 2.2 wt% of (b) graphite, (c) RP, (d) GP2, (e) GP4 or (f) GP6. The PI foams caused flame with different sizes (indicated in figure) when they were burned. Combustion tests of the PI foams containing other contents of the various flame retardants were also performed by this way.

Table S3. Flame-retardant properties of the PI foams containing various quantities of the various flame retardants (indicated).[a]

Loading [wt%]	Pristine graphite	Pristine RP	GP2	GP4	GP6
0	+++	+++	+++	+++	+++
1.6	+++	+++	++	++	++
1.9	+++	++	+	++	++
2.2	+++	++	0	+	+
2.5	+++	++	0	0	+
2.8	+++	+	0	0	0
3.1	+++	0	0	0	0

[a]To further evaluate the flame retardants, PI foams with various loadings of each flame retardant indicated were prepared. The outcomes described in the table are qualitative, and defined on the basis of the sizes and the propagation speeds of the flames produced: +++, the foam tested resulted in significant burning; ++, the foam tested resulted in burning; +, the foam tested resulted in minimal burning; 0, the foam did not burn.

Table S4. LOI values of pristine PI foam and the PI foams containing 2.2 wt% of the various flame retardants (indicated).

Sample	Pristine PI foam	PI foam 2.2 wt% Graphite	PI foam 2.2 wt% RP	PI foam 2.2 wt% GP2	PI foam 2.2 wt% GP4	PI foam 2.2 wt% GP6
LOI [%]	25.9	26.5	37.3	39.4	38.6	37.9

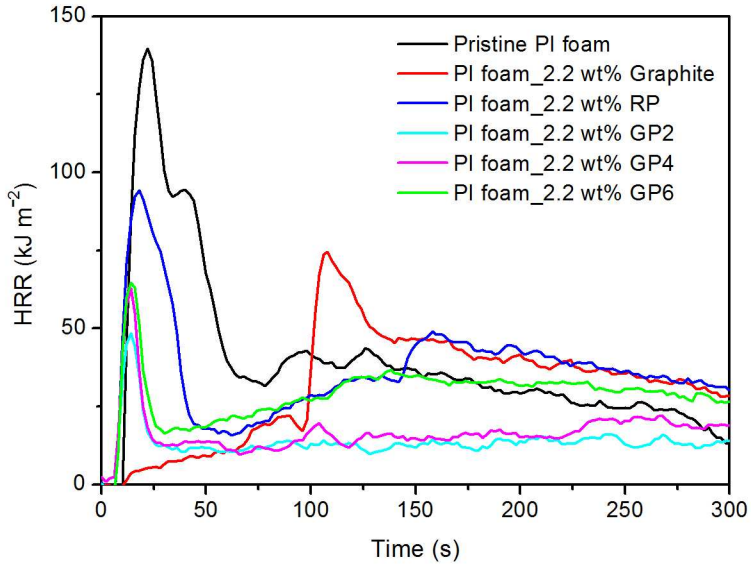

Figure S13. Cone calorimetry tests recorded for a pristine PI foam and the PI foams containing 2.2 wt% of the various flame retardants (indicated).

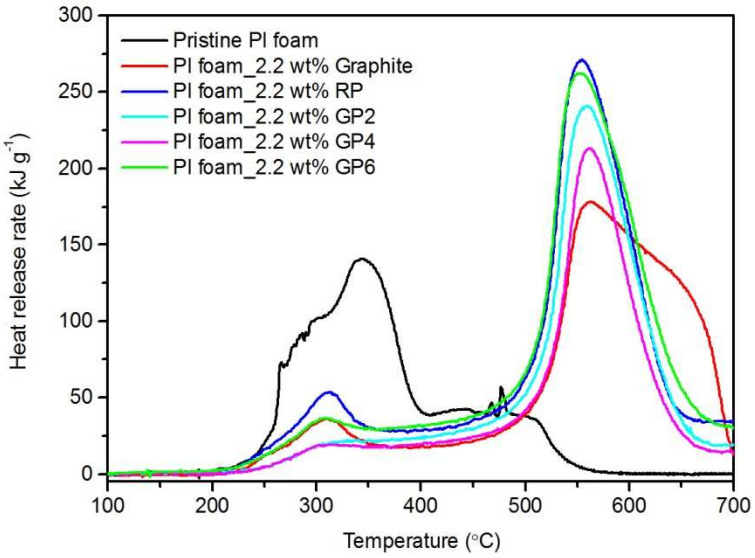

Figure S14. Micro combustion calorimetry tests recorded for a pristine PI foam and PI foams containing 2.2 wt% of the various flame retardants (indicated). The foams were measured under an oxidizing atmosphere (O_2/N_2 = 20/80).

The Micro combustion calorimetry (MCC) data indicated that addition of the various flame retardants significantly enhanced the thermal stabilities of the resultant PI foams by moving the major peak heat release rate (pHRR) to higher temperatures (Figure S14). The foam containing GP2 was found to exhibit markedly a decreased pHRR value (19.7 kJ g^{-1}) and a total heat release (THR) value (3.14 kJ g^{-1}) in the range from 200 to 400 °C, which were only 14.0 and 12.1% of the values measured for the pristine PI foam (140.9 kJ g^{-1} and 25.93 kJ g^{-1}, respectively), indicating a substantially enhanced flame resistance of the GP2-containing PI foams. Significantly, the flame retardancy of the GP2-contianing PI foam is also superior when compared to that of the RP-containing PI foam, as the pHRR and THR values recorded for the former were 36.8 and 51.9% of those recorded for the latter, respectively (Table S5). Note that the pHRR appeared at higher temperatures (ca. 570 °C) in the MCC curves recorded for the flame-retardant PI foams was ascribed to the eventual thermal decomposition of the polymer.

Table S5. Parameters of the PI foams obtained from micro combustion calorimetry (Figure S14).[a]

Sample	T_p [°C]	pHRR [kJ g^{-1}]	THR [kJ g^{-1}]
Pristine PI foam	342.3	140.9	25.93
PI foam_2.2 wt% Graphite	310.5	36.3	3.80
PI foam_2.2 wt% RP	311.1	53.6	6.05
PI foam_2.2 wt% GP2	308.8	19.7	3.14
PI foam_2.2 wt% GP4	309.6	19.3	2.73
PI foam_2.2 wt% GP6	308.7	36.8	5.10

[a]Heat release peaks were observed from 200 to 400 °C and/or from 450 to 650 °C in the heat release rate curves recorded for the PI foams (Figure S14). It is seen that the addition of GPx composites into the PI foams resulted in significantly reduced heat release peaks in the lower temperature region, indicating that the thermo-oxidative stabilities of the foams were improved up to higher than 500 °C.

The heat release peaks observed in the higher temperature region correspond to the final burning of the foams. The parameters shown in the table were derived from the peaks observed in the lower temperature region.

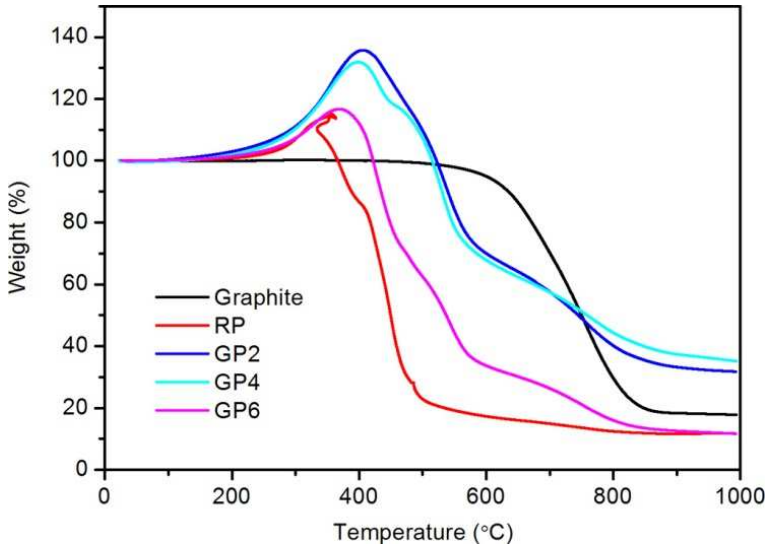

Figure S15. TGA data recorded under an atmosphere of air for graphite, RP and the GPx composites prepared at various RP/graphite ratios.

Table S6. Thermal parameters of RP and the GPx composites as derived from the TGA data that were collected under an atmosphere of air (Figure S15).

Sample	T_{peak} [°C][a]	W_{total} [%][b]	W_{RP} [%][c]	η[d]
RP	354	15.4	15.4	1
GP2	406	35.8	53.6	3.5
GP4	398	31.9	39.9	2.6
GP6	369	16.7	19.5	1.3

[a]T_{peak} represents the temperature corresponding to the maximum mass increase observed. [b]W_{total} represents the percentage of the maximum increase relative to the total mass of the respective material measured. [c]W_{RP} represents the percentage of the maximum increase relative to the mass of RP in the

respective composite. [d] η represents the increased uptake of O_2 with respect to that of pristine RP, which was calculated by dividing the W_{RP} of the composites by that of pristine RP.

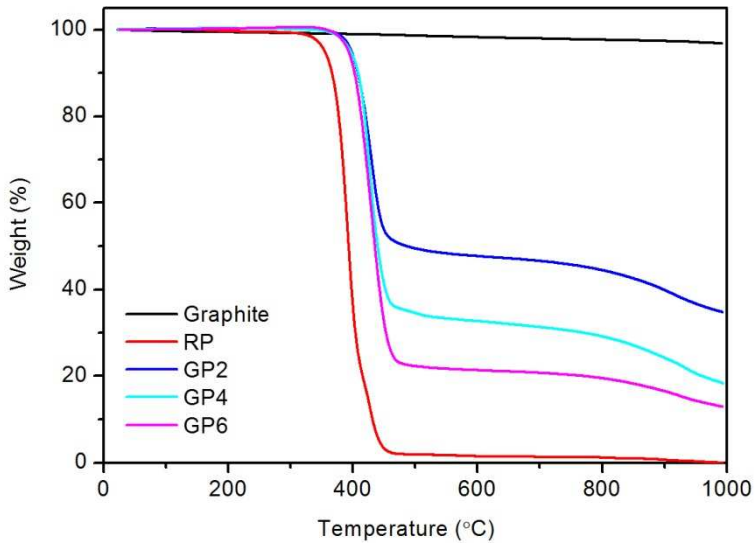

Figure S16. TGA data of graphite, RP and the GPx composites prepared at various RP/graphite ratios. The TGA data were collected under an atmosphere of N_2.

REFERENCES

1. Hayashi, S.; Hayamizu, K. Shift References in High-Resolution Solid-State NMR. *Bull. Chem. Soc. Jpn.* **1989**, *62*, 2429–2430.

2. Eichele, K.; Wasylishen, R. E. ^{31}P NMR Study of Powder and Single-Crystal Samples of Ammonium Dihydrogen Phosphate: Effect of Homonuclear Dipolar Coupling. *J. Phys. Chem.* **1994**, *98*, 3108–3113.

3. Ramireddy, T.; Xing, T.; Rahman, M. M.; Chen, Y.; Dutercq, Q.; Gunzelmann, D.; Glushenkov, A. M. Phosphorus-Carbon Nanocomposite Anodes for Lithium-Ion and Sodium-Ion Batteries. *J. Mater. Chem. A* **2015**, *3*, 5572–5584.

4. Fichera, M. A.; Braun, U.; Schartel, B.; Sturm, H.; Knoll, U.; Jager, C. Solid-State NMR Investigations of the Pyrolysis and Thermo-Oxidative Decomposition Products of a Polystyrene/Red Phosphorus/Magnesium Hydroxide System. *J. Anal. Appl. Pyrolysis* **2007**, *78*, 378–386.

5. Bytchkov, A.; Fayon, F.; Massiot, D.; Hennet, L.; Price, D. L. ^{31}P Solid-State NMR Studies of the Short-Range Order in Phosphorus-Selenium Glasses. *Phys. Chem. Chem. Phys.* **2010**, *12*, 1535–1542.

6. Groh, M. F.; Paasch, S.; Weiz, A.; Ruck, M.; Brunner, E. Unexpected Reactivity of Red Phosphorus in Ionic Liquids. *Eur. J. Inorg. Chem.* **2015**, *24*, 3991–3994.

7. Lange, S.; Schmidt, P.; Nilges, T. Au_3SnP_7@Black Phosphorus: An Easy Access to Black Phosphorus. *Inorg. Chem.* **2007**, *46*, 4028–4035.

8. Boehm, H. P. Surface Oxides on Carbon and their Analysis: A Critical Assessment. *Carbon* **2002**, *40*, 145–149.

9. Ghafuri, H.; Talebi, M. Water-Soluble Phosphated Graphene: Preparation, Characterization, Catalytic Reactivity, and Adsorption Property. *Ind. Eng. Chem. Res.* **2016**, *55*, 2970–2982.